A SEMI-ANALYTICAL METHOD FOR MEASURING THE STRAIN ENERGY RELEASE RATES OF ELLIPTICAL CRACKS

M. Burhan[1*], T. Scalici[2], Z. Ullah[1], Z. Kazancı[1], B.G. Falzon[1,3], G. Catalanotti[1,4]

[1]Advanced Composites Research Group, School of Mechanical and Aerospace Engineering, Queen's University Belfast, Belfast, United Kingdom,
[2]Facoltà di Ingegneria e Architettura, Università degli Studi di Enna Kore, Cittadella Universitaria, Enna, 94100, Italy,
[3]School of Engineering, RMIT University, Melbourne, Australia,
[4]Escola de Ciências e Tecnologia, Universidade de Évora, Colégio Luis António Verney, Rua Romão Ramalho 59, 7000-671 Évora, Portugal
* M. Burhan[1] (mburhan01@qub.ac.uk)

Keywords: Energy release rate (ERR), Virtual Crack Closure Technique (VCCT), Semi-elliptical crack, bi-material laminate

ABSTRACT

In this study, a fracture mechanics analysis is presented to address the concern of delamination propagation at the interface of a bi-material laminate. In general, the energy release rate at the crack front is the fracture parameter required to study the propagation of cracks. A new three-dimensional finite element technique, for the evaluation of the energy release rate along the interfacial semi-elliptical crack front in hybrid composite-metal substrates, is presented. Using a non-dimensional correction factor, the related equation expresses the normalized energy release rate. A non-dimensional function with non-dimensionalized functional groups is utilized to investigate the effects of several factors. These factors include the variation in material stiffness between layers, the relative thickness of the two substrates at whose interface the analysis is performed, and the effects of two semi-axes of a semi-elliptical crack on the analysis of the correction factor. These non-dimensional function values were derived by employing a careful interpolation technique on a set of finite element solutions, yielding predictions that exhibit accuracy within acceptable range of numerical results.

1 INTRODUCTION

The interface of two dissimilar materials, with no through-thickness reinforcement, is often the weakest part of the composite structures, which may ultimately restrict the application of layered structures. Consequently, the study of delamination initiation and propagation at such interfaces has received considerable attention. Early pioneering investigations on an interface crack between two dissimilar linear elastic, isotropic, and homogeneous materials was conducted by Williams [1], Rice and Sih [2,3] and others [4,5]. They found an oscillating behavior of stresses and the physically impossible interpenetration of two crack faces close to the crack tip. To overcome the inconsistencies observed in the Stress Intensity Factor (SIF) approach, it was proposed in [6] to use energy release rate (ERR) as a characterizing parameter for interfacial crack problems. Wang and Choi [7,8] studied the interfacial crack behavior in anisotropic composites under mixed mode loading using partially closed interface crack model.

The bi-material interface fracture causes opening, shearing, and tearing mode, even for a single mode of loading, as opposed to crack problems in homogenous materials. Therefore, the interface fracture toughness, denoted as $\mathcal{G}_c$, becomes crucial to quantify as a function of mode-mixity, given that the crack propagation occurs under mixed mode conditions. The development of several test specimens for determining interface fracture toughness may be seen in the works of Hutchinson and Suo [9], Wang and Suo [10], and other's [11,12]. All these specimens are used to assess the interface toughness of 2D

plane stress or plane strain bi-material systems in mixed mode I and II. For three-dimensional interface cracks the analytical solution for the complex SIFs of a penny-shaped crack embedded in an infinite solid subjected to remote tension was established in [13]. Enriched Finite Element Analysis (FEA) were employed in Ref.[14] to examine the behaviour of semi-circular surface cracks and quarter-circular corner cracks, while the virtual crack closure method was utilized to assess corner interface crack issues in [15]. Other numerical techniques which have been proposed in the literature are scaled boundary finite-element methods [16], extended finite elements [17], and boundary finite-element methods [18]. However the above works have primarily focused on specific three-dimensional cracks, while a significant number of structural components exhibit semi-elliptical cracks [19].

In this study, a semi-elliptical bi-material interface edge crack in a laminate, under remote tensile load, is investigated for fracture mechanics assessments. Preliminary dimensional analysis is conducted to investigate the parameters influencing ERR at the three-dimensional interface semi-elliptical edge crack in a bi-material system. 3D Virtual crack closure technique (3D VCCT) was used to calculate ERRs along the crack front and a detailed three-dimensional FEA is conducted. The FEA model is used to develop a new comprehensive three-dimensional semi-analytical method for calculating ERR distributions in mode I, II, and III for general and symmetric laminate interfaces with any given material system and geometry. Subsequently, effects of variation in elastic properties of substrates, geometry, and crack dimensions on ERRs distribution is also studied.

2 ANALYTICAL MODEL

In Figure 1, a general laminate configuration is depicted. It features a 3D interface semi-elliptical edge crack and the illustration is of an Edge Delamination Specimen (EDS) coupon. The laminate dimensions are, length $L = 75H$, and width $2W = 15H$. The two substrates are referred to as *master layer* and *slave layer*. The bottom *master* and top *slave layer* substrate have H and h thickness, respectively. The *master layer* is modelled as linear elastic, homogenous, and transversely isotropic material with orientation as 90°, while as the *slave layer* as linear elastic and isotropic. When the laminate is subjected to loading in displacement control δ, the reaction forces can be used to calculate remote stress σ_{∞}. This stress gives rise to a three-dimensional stress concentration near free edge of the laminate. In the EDS coupon, due to this stress the crack becomes subjected to a mixed-mode fracture scenario, involving mode I, II, and III.

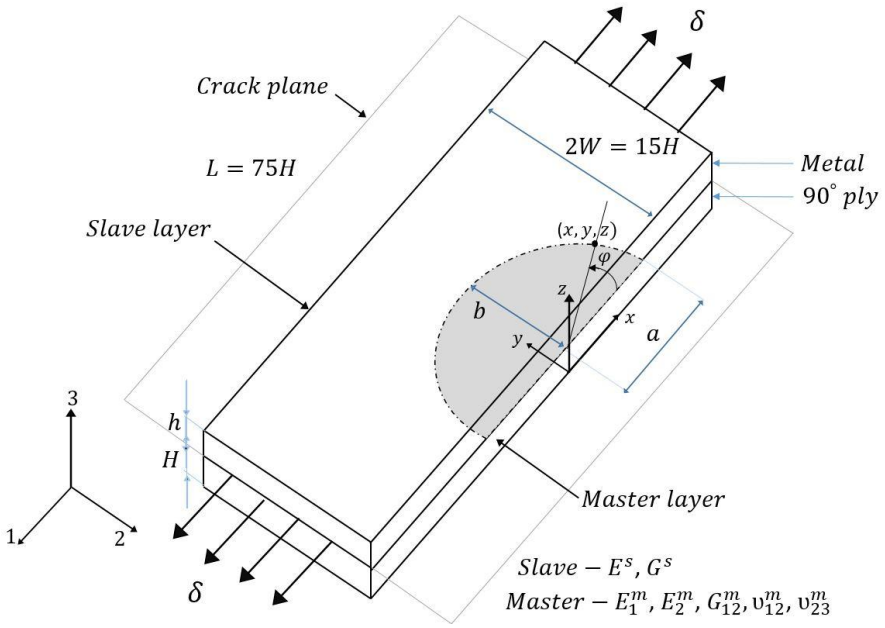

Figure 1: Edge Delamination Specimen (EDS) coupon with a semi-elliptical edge crack at the interface of a bi-material laminate.

The mode-mixity is determined with respect to a vector normal to the crack front and varies with polar angle ϕ. Crack dimensions a and b are here defined as the semi-axes of a semi-elliptical pre-crack at the interface of two substrates (in gray). Global coordinates of the laminates are represented with xyz-axes, where x, y are in-plane and z out-of-plane directions respectively and is situated at the bottom surface of the *master layer*. The 3D interface crack is assumed to be contained in the plane parallel to the load direction at the interface of the *master* and *slave layers*. Under this assumption, an infinite number of crack geometries is still possible. Therefore, a range of a and b is therefore considered within the limits of laminate geometry to study its influence on fracture mechanics parameters.

2.1 Material model

A wide range of materials with variation in material stiffness between *master* and *slave layers* is considered to study the effect of it on fracture parameters. This investigation encompasses a class of carbon-based reinforced composites for *master layer* and a class of metals for *slave layer*. Material invariant, *trace*, $\Im$, defined as an invariant of stiffness and compliance tensors [20] is exploited.

Trace is a fundamental material property as other elastic constants and is an invariant to ply orientation, stacking sequence, loading condition, coordinate transformation, and total number of layers. Classical Laminate Theory (CLT) is used to generate *trace*-normalized stiffness components of several carbon fibre-reinforced polymer (CFRP) laminates. **A Reference Ply** can be defined by using the mean values of these components.

The value of *trace* can be determined using the longitudinal Young's modulus of a 0° unidirectional laminate, E_1, by dividing it by the corresponding *trace*-normalised **Reference Ply** stiffness component, E_1^*,

$$\Im = \frac{E_1}{E_1^*}. \tag{1}$$

Since *traces* exist for all tensors, the general 3D stiffness *traces* were utilized for CFRP. Based on the general 3D *trace*-normalized stiffness components of the **Reference Ply**, C_{ij}^*, the 3D stiffness components of the any laminate can be determined according to

$$C_{ij} = C_{ij}^* \, \Im, \tag{2}$$

where $\Im$ represents the *trace* of the 3D stiffness matrix $[C]$ in this study unless stated otherwise. The compliance matrix is calculated by taking the inverse of $[C]$ and the engineering constants ($E_1, E_2, \upsilon_{12}, G_{12}, \upsilon_{23}$) of the laminates are subsequently determined.

The purpose of employing the *trace* theory in this study is to streamline the process by inputting only the **Reference Ply** *trace*-normalised factors and *traces* of all laminates in the Finite Element Method (FEM) model, instead of individual engineering constants for each material. This approach aims to determine the elastic constants of laminates more efficiently.

2.2 Dimensional analysis

The ERR $\mathcal{G}$ for a general bi-material laminate as shown in Figure 1 depends, a priori, on the set of parameters such as remote stress σ_∞, elastic properties of *master* ($E_1^m, E_2^m, G_{12}^m, \upsilon_{12}^m, \upsilon_{23}^m$) and *slave* ($E^s, G^s$) *layers*, the thickness of *master layer* H and *slave layer* h, the polar angle ϕ, and crack $(a, b, location)$ and laminate (W, L) geometries. Therefore, the ERR $\mathcal{G}$ distribution is an unknown function of the following parameters

$$\mathcal{G} = \mathcal{G}\begin{pmatrix}(\sigma_\infty), (a, b, location), (\phi), (h, H, W, L), \\ (E^s, G^s), (E_1^m, E_2^m, G_{12}^m, \upsilon_{12}^m, \upsilon_{23}^m)\end{pmatrix}. \tag{3}$$

The elastic properties of two substrates in a laminate can be represented by their *traces* $\Im_m$ for *master layer* and $\Im_s$ for *slave layer*, which are normalised with reference values $\Im_m^*$ and $\Im_s^*$. It is noted here that $\Im_s$ represents the *trace* of 2D stiffness matrix $[Q]$ for a metal-based materials and are listed in Table 1 along with the corresponding elastic properties.

The reference values used here for the *master layer* is $\Im_m^* = 200\ GPa$, which is close to the mean value of a range of carbon-based composites considered, and for the *slave layer*, this is $\Im_s^* = 320\ GPa$,

that of titanium. If the location of a crack is at a free edge in the middle of a laminate along the length and a very long EDS coupon is considered where ($L \gg a, H$) and ($2W \geq 3b$), then following sequential elimination, Eq. (3), in terms of non-dimensional groups, can be written as

$$\pi_{\mathcal{G}} = \pi_{\mathcal{G}}\left(\frac{\mathcal{G}E'}{{\sigma_\infty}^2 h}, \omega, \mu, \eta, \alpha, \beta, \phi\right), \tag{4}$$

where $E' = \Im_m.\omega/\mu$ (equivalent modulus), $\omega = \Im_m/\Im_m^*$ and $\mu = \Im_s/\Im_s^*$ (the normalised material parameters), $\eta = H/h$ (the relative thickness), and $\alpha = a/H$ and $\beta = b/H$ (the normalised crack semi-axes). Finally, the ERR distribution along the semi-elliptical crack front for an arbitrary combination of parameters for a given stacking sequence in a bi-material system may be determined using

$$\mathcal{G}_i(\omega, \mu, \eta, \alpha, \beta, \phi) = \frac{{\sigma_\infty}^2 h}{E'}\psi_i^2(\omega, \mu, \eta, \alpha, \beta, \phi), \qquad i \in \{I, II, III\}, \tag{5}$$

where ψ is a non-dimensional correction factor and subscripts (I, II, III) refer to different modes of fracture.

For a given bi-material laminate without solving for an analytical solution or boundary finite element method, different general laminate configurations can be examined efficiently saving much numerical effort by calculating the correction factor function ψ only once.

Material	$E(GPa)$	υ	Ref	$G(GPa)$	$\Im_s(GPa)$	μ
Aluminium7075-T6	71.7	0.33	[21]	27	215	0.672
Titanium-Grade 2	105	0.37	[22]	38.3	320	1
Steel DP-700	207	0.29	[23]	80.2	612	1.913

Table 1: Elastic properties of metals considered for *slave layer* with their 2D *traces* and references

4 NUMERICAL MODEL

For the laminate illustrated in Figure 1, the three-dimensional model with the 8-node 3D linear brick, reduced integration element, C3D8R was used. The ERR distributions in all modes along the crack front is calculated by the Abaqus built-in procedure 3D VCCT. It is a numerical technique that assumes that the required energy to fracture a unit surface area is equal to the energy required to close it. It also assumes the crack propagation along a predefined path.

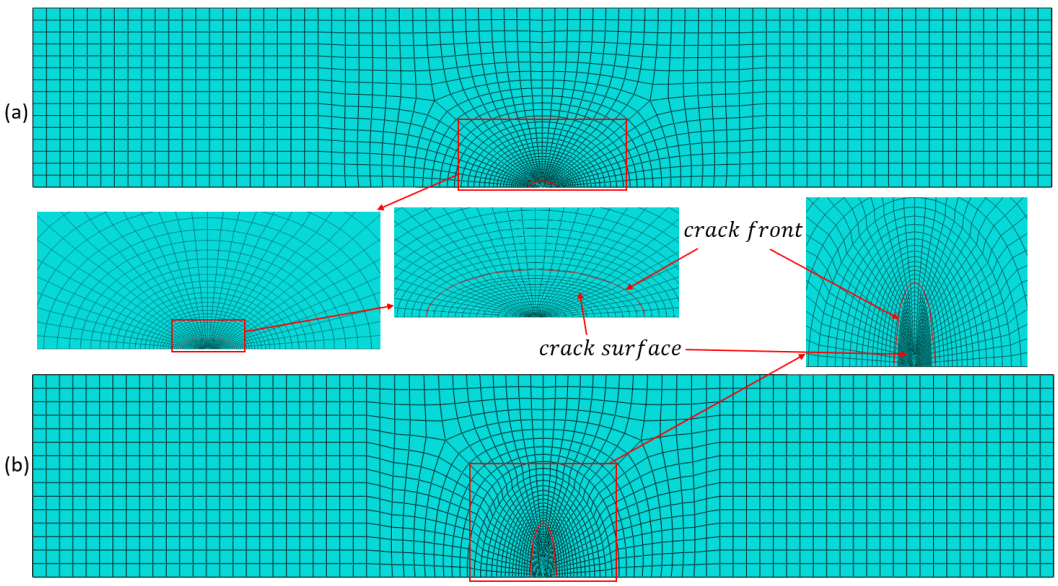

Figure 2: A typical magnified orthogonal (almost) mesh around semi-elliptical crack for two crack configurations: (a) $\alpha = 1, \beta = 0.5$, and (b) $\alpha = 1, \beta = 4$.

It is important to note that to consider the varying fracture modes direction along the semi-elliptical crack front, a local coordinate system needs to be defined at each node along the contour of the crack. This is necessary because the fracture mode direction constantly varies along the crack front with polar angle ϕ.

In the present study, one focus was to understand the effects of infinite possible crack configurations that can exist within the interface of bi-material laminate on fracture parameter ERR distribution. It is extremely difficult to maintain an orthogonal mesh at the crack front for any given crack configurations, which is normally required for 3D VCCT [24]. To deal with the corresponding non-orthogonality issue, a careful and strict consideration was made for the meshing. The non-orthogonality of the mesh was adjusted in an area within the crack surface behind the crack front. Hence, due to this reason an almost orthogonal mesh is obtained in radial segments along the crack front for any given configuration of the crack. Meshes of such two crack configurations which have one semi-axis longer than the other, is presented in Figure 2 (a) for $\alpha = 1, \beta = 0.5$, and in (b) for $\alpha = 1, \beta = 4$. Given the focus of the present research which is studying the fracture parameters in 3D interface crack in bi-material systems, it is assumed that the region of crack surface where non-orthogonality is corrected does not influence the ERR components at the crack front. This approach was found to effectively mitigate the non-orthogonality issue in the semi-elliptical cracks, resulting potentially in an improvement in the accuracy of the ERR calculation.

5 RESULTS

In this section, a novel three-dimensional semi-analytical method for calculating components of the ERR along the semi-elliptical crack front at the interface in bi-material laminates is presented. The ERR components distribution exhibit a linear dependence on the square of remote stress for given parameters within a linear elastic region. This observation is exploited in this paper by finding these non-dimensionalised function distributions only once for all combinations of parameters based on reasonable ranges chosen. Therefore, different laminate configurations with different materials and geometry can be examined efficiently saving numerical effort.

The ERR components are initially computed using VCCT for the material parameters $\omega \in \{0.825 - 1.225\}$, $\mu \in \{0.672 - 1.913\}$, and geometric parameter $\eta \in \{0.7 - 1.3\}$, with additional crack parameters $\alpha \in \{0.1 - 7\}$, and $\beta \in \{0.08 - 5\}$. The components were calculated for the given range of parameters using the numerical model (implemented in a python script and FEA carried out in Abaqus) developed for a metal-unidirectional composite (90°) bi-material laminate. Based on these values, correction factors for the same parameter combinations was calculated using

$$\psi_i(\omega, \mu, \eta, \alpha, \beta, \phi) = \frac{1}{\sigma_\infty}\sqrt{\frac{\mathcal{G}_i E'}{h}}. \tag{6}$$

The effects of parameters on these non-dimensionalised correction factor components for a given ranges was then investigated.

By determining these non-dimensionalised functions, a significant amount of numerical effort can be saved in analysing the behaviour of three-dimensional interface semi-elliptical cracks in bi-material laminates for any set of parameters, as they only need to be determined once. Since all the possible combinations of parameters were considered to calculate corresponding non-dimensionalised functions, the output data results in a large dataset with high resolution. To obtain the ERRs for any given combination of input parameters, Delaunay's tessellation was used in the post-processing stage. This enabled the use of linear interpolation to extract the ERR distribution for any combination of parameters within the dataset. The method thus eliminates the need for repeated FEA simulations for different parameter combinations.

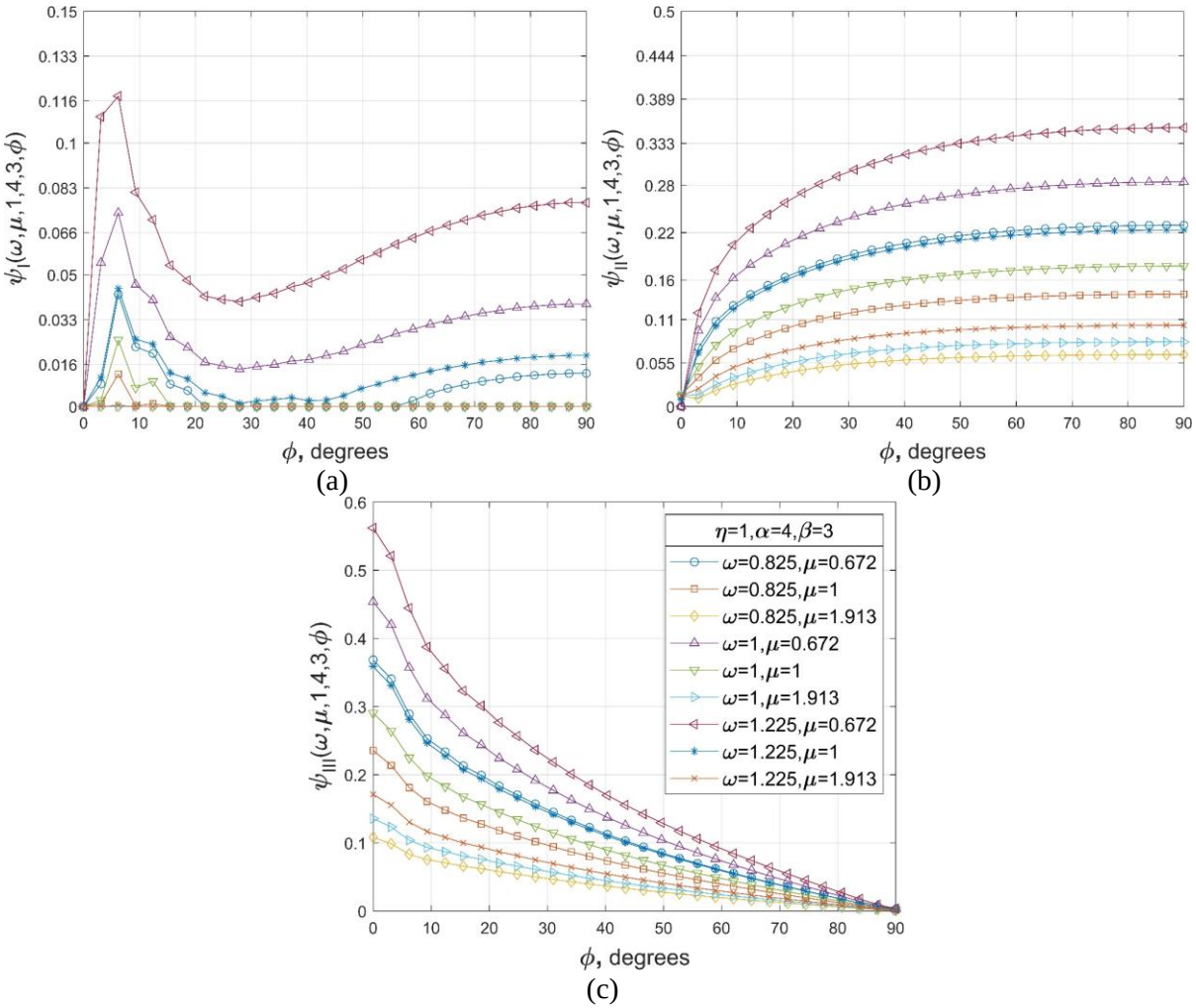

Figure 3: Effect of material parameters ω, and μ on correction factors in all (a) I/ (b) II/ and (c) III fracture modes at the crack front for a given combination of rest of the parameters in $[metal/90]$ bi-material laminate.

The influence of ω, and μ on correction factors distribution along the crack front are presented in Figure 3 (a) mode I, ψ_I, (b) mode II, ψ_{II}, and (c) mode III, ψ_{III} for a given geometric parameter $\eta = 1$, and crack parameters $\alpha = 4$, $\beta = 3$. The ψ_I, ψ_{II} and ψ_{III} distributions exhibit similar behavior, as all decrease significantly with increasing μ when ω is held constant and increase with increasing ω when μ is held constant. Although, all three correction factors are significantly influenced by material parameters, the mode I contribution seems to be insignificant to the total ERR.

Furthermore, the correction factors distribution along the crack front in all three modes for a fixed material parameters $\omega = 0.825$, and $\mu = 1$, and crack parameters $\alpha = 4$, $\beta = 3$ are found to be uniformly influenced when η is increased. Figure 4 (a) shows the distribution of ψ_I, (b) shows ψ_{II}, and (c) shows ψ_{III}. It is observed that all correction factors increase with an increase in η, indicating that the ERR components distribution increases as the thickness of the *metal (slave) layer* decreases by keeping the *composite (master) layer* constant.

The effect of crack parameters α, and β on correction factors along the crack front for a given material parameters $\omega = 0.825$, $\mu = 1$, and geometric parameter $\eta = 1$ are shown in Figure 5 (a) ψ_I, (b) ψ_{II}, and (c) ψ_{III}. In this current case the influence of α, β is also studied on total ERR $\mathcal{G}_T$, which can be written as $\mathcal{G}_T = \mathcal{G}_I + \mathcal{G}_{II} + \mathcal{G}_{III}$, and the corresponding correction factor ψ_T as $\psi_T = \sqrt{\psi_I^2 + \psi_{II}^2 + \psi_{III}^2}$. Figure 5 (d) illustrates the ψ_T distribution. The surfaces plots correspond to $\beta \in \{1, 2.5, 5\}$ are illustrated only for clarity.

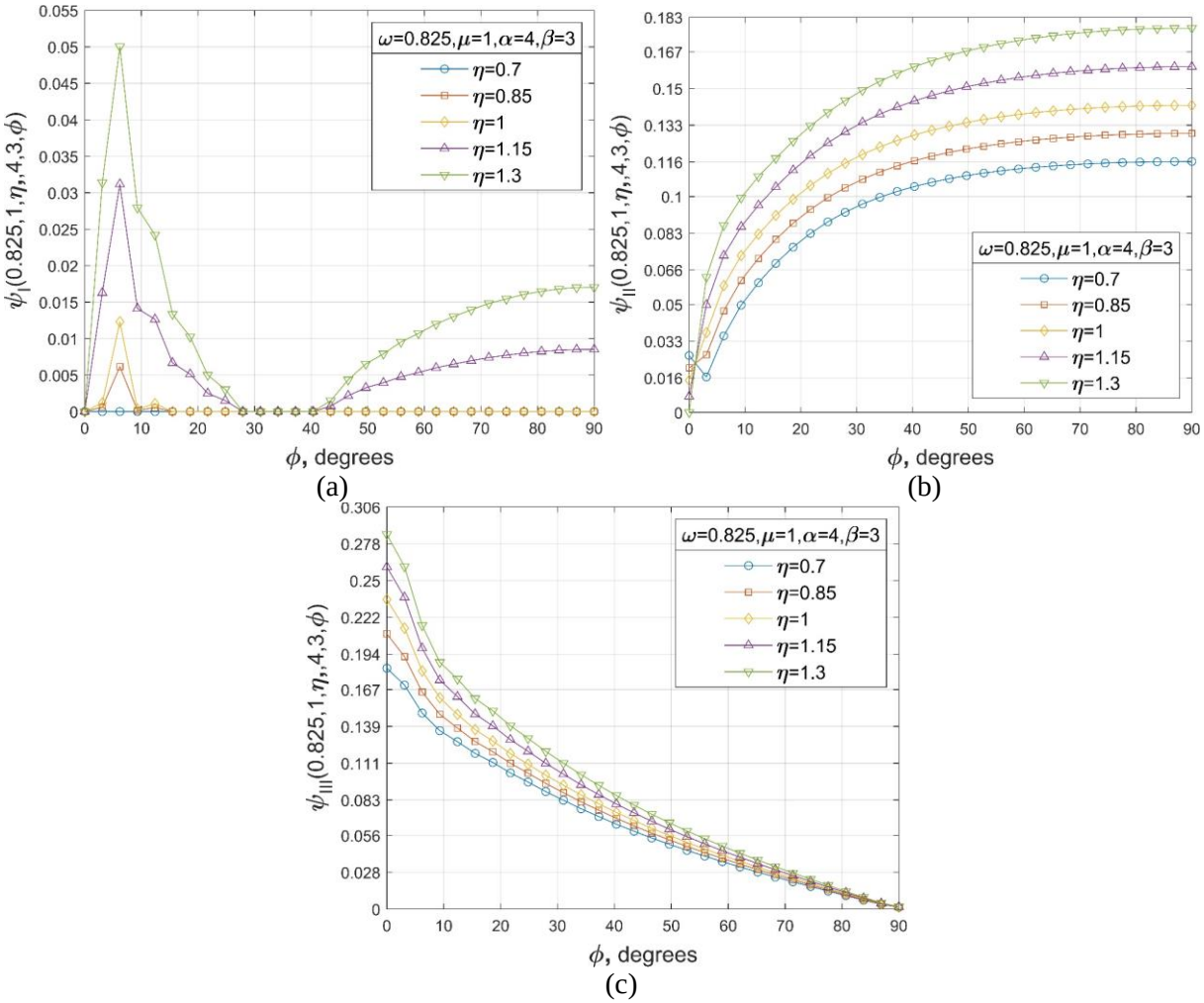

Figure 4: Effect of relative thickness parameter η on correction factors in all (a) I/ (b) II/ and (c) III fracture modes at the crack front for a given combination of rest of the parameters in $[metal/90]$ bi-material laminate.

The behavior of ψ_I, ψ_{II}, and ψ_{III} differs from that of ψ_T. The ψ_{II} decreases as β increases and increases as α increases. Conversely, the ψ_I and ψ_{III} increases as β increases and decreases as α increases. This behavior was expected, when the crack configuration has one larger semi-axis α than β, most of the crack front will go into mode II and less into mode III. As the maximum portion of the crack will have more influence of the fracture component that is normal to the crack front in the delamination plane. The opposite applies when α is significantly smaller than β, and mode III will prevail. Of course, this observed dominance of modes when one semi-axis is larger than the other may vary when there are changes in the stacking sequence of the laminate.

It is observed that, as β increases, the ψ_T increases near the polar angle $\phi = 0^\circ$ for a given α and decreases in the region far away from this point. On the other hand, increasing α results in a decrease in the ψ_T distribution near $\phi = 0^\circ$ in general and an increase in the region far away from it, leading to the presence of crossover curves in the surface plots. These curves were found to be present in the range of $\phi \in \{5^\circ - 50^\circ\}$. In general, when α is increased, the ψ_T increases, and when β is increased, the ψ_T distribution increases near the free edge and decreases away from it. In addition to that, $\mathcal{G}_{II}$ was observed to demonstrate similar behaviour as ψ_T in less than $\phi \in \{10^\circ\}$.

It is noteworthy here to mention that the mode I contribution is insignificant throughout the crack front in all parametric studies.

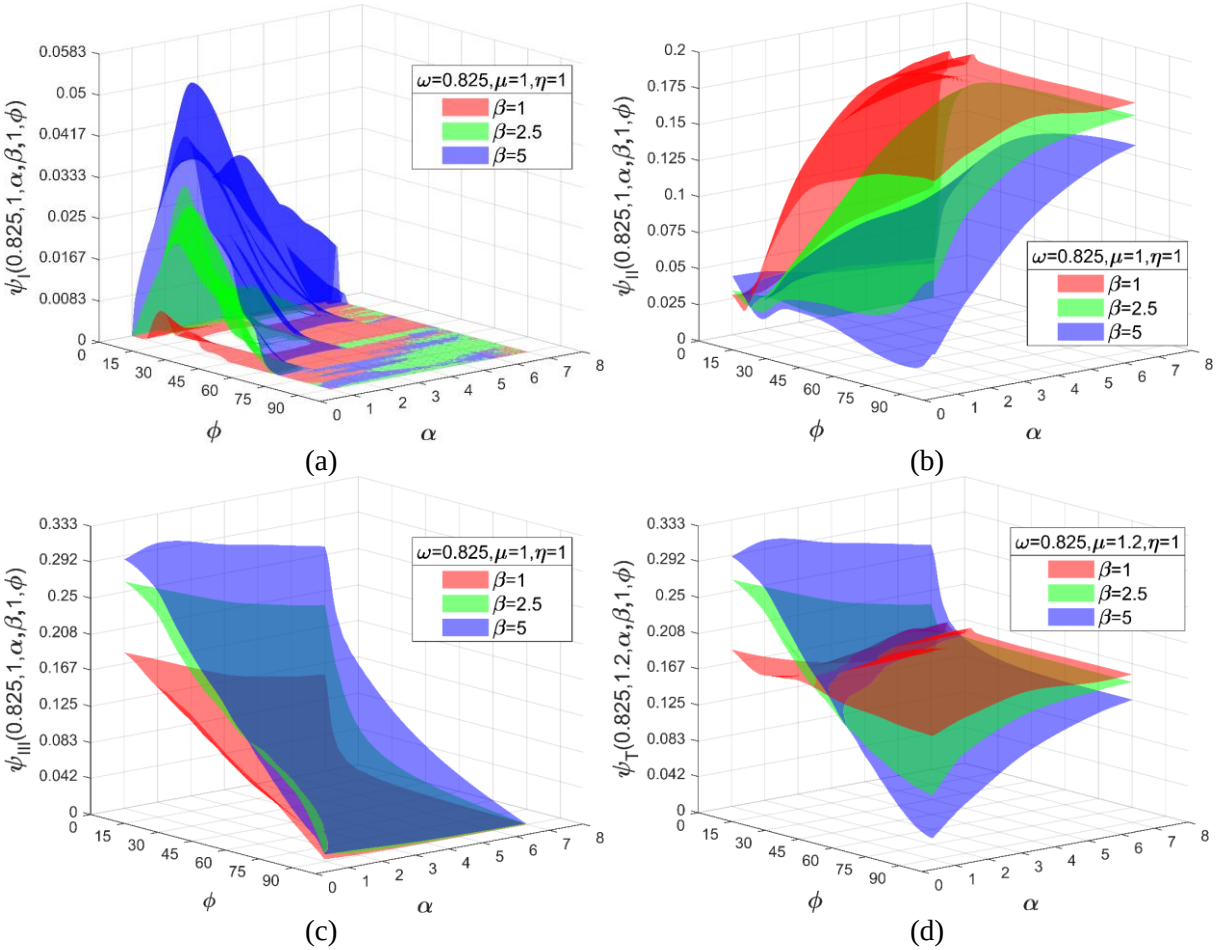

Figure 5: Effect of normalised crack dimensions on correction factor in (a) mode *I*, (b) mode *II*, (c) mode *III*, and (d) total for a given combinations of material and geometry parameters.

9 CONCLUSIONS

This study presents a semi-analytical method to calculate the energy release rate (ERR) component distribution along the 3D interface semi-elliptical crack front in a bi-material laminate with orientation [metal/90°]. The method considers a class of carbon-based composites and metals, where two material parameters were defined based on material *traces*, and one for representing a relative ply thickness of two substrates in a bi-material laminate. The method also accounts for two normalized crack parameters influence on ERR distribution. A preliminary dimensionality reduction of ERR distribution is performed, and non-dimensional functions are identified, which depend on functional groups of material, geometric, and crack parameters.

To evaluate ERR, 3D-VCCT was utilized and a numerical model was developed. The non-dimensionalised functions were found to be independent of remote extension and subsequently were used in the development of a new semi-analytical method to calculate the ERR distribution at the bi-material interface. This method was used to study the influence of material, geometric, and crack parameters on these correction factor components. The study of the ERR component distribution influenced by crack parameters revealed that mode *II* increases when the normalized longitudinal semi-axis α of semi-elliptical crack increases and decreases when the transverse semi-axis β increases. In contrast, mode *III* increases when α decreases and increases when β increases. Correction factors belonging to total ERR behave differently than other modes. In general, the distribution increases with an increase in α and decreases with an increase in β, leading to crossover points in distribution.

This method can be used to study interface fracture assessments for a given bi-material laminate. Since this study was performed on a fixed orientation of a *composite (master) layer*, the parameters belonging to the material orientation can be introduced to make the semi-analytical model more generalized. The

non-dimensionalised functions need to be determined for a specific combination of parameters with adequate resolution in data to capture any notable sudden changes that may occur within the intermediate range of the parameters.

ACKNOWLEDGEMENTS

This study was conducted as part of the Belfast Maritime Consortium UKRI Strength in Places project, 'Decarbonisation of Maritime Transportation: A return to Commercial Sailing' led by Artemis Technologies, Project no. 107138.

REFERENCES

[1] M. L. Williams. The stresses around a fault or crack in dissimilar media. Bull Seismol Soc Am 1959;49:199–204.

[2] Sih GC, Rice JR. The bending of plates of dissimilar materials with cracks. J Appl Mech Trans ASME 1964;31:477–82. https://doi.org/10.1115/1.3629665.

[3] Rice JR, Sih GC. Plane Problems of Cracks in Dissimilar Media. J Appl Mech 1965;32:418–23. https://doi.org/10.1115/1.3625816.

[4] Erdogan F. Stress Distribution in Bonded Dissimilar Materials With Cracks. J Appl Mech 1965;32:403–10. https://doi.org/10.1115/1.3625814.

[5] England AH. A crack between dissimilar media. J Appl Mech 1965:400–2. https://doi.org/10.1016/0020-7225(71)90055-3.

[6] Mulville DR, Mast PW, Vaishnav RN. Strain energy release rate for interfacial cracks between dissimilar media. Eng Fract Mech 1976;8:555–65. https://doi.org/10.1016/0013-7944(76)90009-6.

[7] Wang SS, Choi I. The interface crack between dissimilar anisotropic composite materials. J Appl Mech Trans ASME 1983;50:169–78. https://doi.org/10.1115/1.3166986.

[8] Wang SS, Choi I. The interface crack behavior in dissimilar anisotropic composites under mixed-mode loading. J Appl Mech Trans ASME 1983;50:179–83. https://doi.org/10.1115/1.3166987.

[9] Hutchinson JW, Suo Z. Mixed mode cracking in layered materials. Adv Appl Mech 1991;29:63–191.

[10] Sou ZW. Experimental determination of interfacial toughness curves using brazil-nut-sandwiches. Acta Met 1990;38:1279–90.

[11] O'Dowd N, Shih CF, Stout MG. Test geometries for measurng interfacial fracture toughness. Int J Solids Struct 1992;29:571–89.

[12] Banks-Sills L, Travitzky N, Ashkenazi D, Eliasi R. A methodology for measuring interface fracture properties of composite materials. Int J Fract 1999;99:143–60.

[13] Kassir M, Bregman A. The stress intensity factor for a penny- shaped crack between two dissimilar materials. J Appl Mech 1972;39:308–10.

[14] Ayhan AO, Kaya AC, Nied HF. Analysis of three-dimensional interface cracks using enriched finite elements. Int J Fract 2006;142:255–76. https://doi.org/10.1007/s10704-006-9040-7.

[15] Chiu TC, Lin HC. Analysis of stress intensity factors for three-dimensional interface crack problems in electronic packages using the virtual crack closure technique. Int J Fract 2009;156:75–96. https://doi.org/10.1007/s10704-009-9348-1.

[16] Song C, Wolf JP. Semi-analytical representation of stress singularities as occurring in cracks in anisotropic multi-materials with the scaled boundary finite-element method. Comput Struct 2002;80:183–97. https://doi.org/10.1016/S0045-7949(01)00167-5.

[17] Nagashima T, Omoto Y, Tani S. Stress intensity factor analysis of interface cracks using X-FEM. Int J Numer Methods Eng 2003;56:1151–73. https://doi.org/10.1002/nme.604.

[18] Gao YL, Tan CL, Selvadurai APS. Stress intensity factors for cracks around or penetrating an

elliptic inclusion using the boundary element method. Eng Anal Bound Elem 1992;10:59–68. https://doi.org/10.1016/0955-7997(92)90079-M.

[19] Liu Z, Chen X, Yu D, Wang X. Analysis of semi-elliptical surface cracks in the interface of bimaterial plates under tension and bending. Theor Appl Fract Mech 2017. https://doi.org/10.1016/j.tafmec.2017.07.019.

[20] Tsai SW, Melo JDD. An invariant-based theory of composites. Compos Sci Technol 2014;100:237–43. https://doi.org/10.1016/j.compscitech.2014.06.017.

[21] Al-Rifaie H, Sumelka W. The development of a new shock absorbing uniaxial graded auxetic damper (UGAD). Materials (Basel) 2019;12. https://doi.org/10.3390/ma12162573.

[22] Catherine LDK, Abdul Hamid D Bin. The effect of heat treatment on the tensile strength and ductility of pure titanium grade 2. IOP Conf Ser Mater Sci Eng 2018;429:6–11. https://doi.org/10.1088/1757-899X/429/1/012014.

[23] Raeisi S, Tapkir P, Tovar A, Mozumder C, Xu S. Multi-material topology optimization for crashworthiness using hybrid cellular automata. SAE Tech Pap 2019;2019-April. https://doi.org/10.4271/2019-01-0826.

[24] Krueger R. Virtual crack closure technique: History, approach, and applications. Appl Mech Rev 2004;57:109–43. https://doi.org/10.1115/1.1595677.